Computational Electromagnetics

Assignment 3

Rectangular and Ridge Waveguides by Finite Elements

I. Preliminaries

TE^z Modes

Refer to the class slides on the topic of finite element method, Pg 110 onwards. In that formulated treatment for solving the eigenvalues of a rectangular waveguide, the TE^z case was assumed, where $E_z = 0$ and $H_z \neq 0$, and the $[U]$ column vector with elements U_1, U_2, …, U_{16} (being global node values) are from $H_z(x,y) = U(x,y) = \sum_{e=1}^{N_e} \sum_{i=1}^{3} \underbrace{U_i^e}_{\substack{local\\ node\\ values}} N_i^e(x,y)$. Thus, the U_i are generally non-zero on the metallic PEC boundaries of the waveguide, implying that the global nodes U_1, U_2, U_3, U_4, U_5, U_8, U_9, U_{12}, U_{13}, U_{14}, U_{15}, and U_{16}, all being on the boundary of the waveguide PEC walls, must be included in the matrix equation on Pg 137 of the class slides, since H_z is generally non-zero (need not vanish) on the PEC surface. Nevertheless, the Neumann boundary condition: $\hat{n} \cdot \nabla \underbrace{U(x,y)}_{\substack{H_z(x,y)\\ \text{for TE}}} = \frac{\partial U}{\partial n} = 0$ applies in TE^z cases, implying that the boundary term $\oint_{C_s} p(x,y) N_j^e(x,y) [\hat{n} \cdot \nabla \underbrace{U(x,y)}_{\substack{H_z(x,y)\\ \text{for TE case}}}] d\ell$ in Eq. (57) Pg 69 of the class slides vanishes along the boundary contour C_s or C, thus permitting the A_{ij}^e in (59a) Pg 70 of slides to be free from this boundary condition term, and subsequently allowing the matrix equation on Pg 137 of the slides to be free from it as well.

TM^z Modes

However, when it comes to the TM^z case ($H_z = 0$ and $E_z \neq 0$), things are different. Firstly, the boundary U_i values [being the E_z values, since now, $E_z(x,y) = U(x,y) = \sum_{e=1}^{N_e} \sum_{i=1}^{3} U_i^e N_i^e(x,y)$] being the same U_1, U_2, U_3, U_4, U_5, U_8, U_9, U_{12}, U_{13}, U_{14}, U_{15}, and U_{16} global nodes of the figure on Pg 111 of slides (placed here as Fig. 1), must now vanish on the PEC guide walls. Thus, these boundary global nodes may be omitted from the matrix equation on that Pg 137. However this time with TM case, the quantity $\hat{n} \cdot \nabla \underbrace{U(x,y)}_{\substack{E_z(x,y)\\ \text{for TM}}} = \frac{\partial U}{\partial n}$ does not in general vanish, meaning that the

boundary-condition term $\oint_{C_s} p(x,y)N_j^e(x,y)[\hat{n}\cdot\nabla\underbrace{U(x,y)}_{\substack{E_z(x,y)\\ \text{for TM case}}}]d\ell$ in Eq. (57) Pg 69 of the class slides need no longer vanish along the boundary contour. Thus, the A_{ij}^e in (59a) Pg 70 of the slides must no longer be free from this boundary condition term, and same for the matrix equation on Pg 137 of the slides. Therefore, for elements e = 1, 2, 3, 4, 5, 6, 7, 8, 11, 12, 13, 14, 15, 16, 17, and 18 (all elements with nodes at the boundary of the PEC waveguide) of Fig. 1, their elemental matrix equations must be modified to the following:

For e = 1, with all nodes attached to the boundary

$$\left\{\begin{bmatrix} A_{11}^1 & A_{12}^1 & A_{13}^1 \\ A_{21}^1 & A_{22}^1 & A_{23}^1 \\ A_{31}^1 & A_{32}^1 & A_{33}^1 \end{bmatrix}+\begin{bmatrix} ep_{11}^1 & ep_{12}^1 & ep_{13}^1 \\ ep_{21}^1 & ep_{22}^1 & ep_{23}^1 \\ ep_{31}^1 & ep_{32}^1 & ep_{33}^1 \end{bmatrix}\right\}\begin{bmatrix} U_1 \\ U_2 \\ U_5 \end{bmatrix}=\begin{bmatrix} 0 \\ 0 \\ 0 \end{bmatrix} \tag{1a}$$

for which

$$\sum_{e=1}^{N_e}\sum_{i=1}^{3}U_i^e\left\{\overbrace{\iint_{\Omega^e}\left[-p(x,y)\nabla N_j^e(x,y)\cdot\nabla N_i^e(x,y)+k_0^2q(x,y)N_j^e(x,y)N_i^e(x,y)\right]dxdy}^{A_{ij}^e}\cdots\right.$$
$$\left.\cdots+\underbrace{\oint_C p(x,y)N_j^e(x,y)\left[\hat{n}\cdot\nabla N_i^e(x,y)\right]d\ell}_{ep_{ij}^e}\right\} \tag{2}$$
$$=\iint_{\Omega^e}N_j^e(x,y)\,f(x,y)dxdy$$

for j = 1, 2, and 3.

Likewise for the rest:

For e = 2, with only its nodes #1 and 3 attached to the boundary.

$$\begin{bmatrix} 0 \\ 0 \\ 0 \end{bmatrix}=\left\{\begin{bmatrix} A_{11}^2 & A_{12}^2 & A_{13}^2 \\ A_{21}^2 & A_{22}^2 & A_{23}^2 \\ A_{31}^2 & A_{32}^2 & A_{33}^2 \end{bmatrix}+\begin{bmatrix} ep_{11}^2 & ep_{12}^2 & ep_{13}^2 \\ 0 & 0 & 0 \\ ep_{31}^2 & ep_{32}^2 & ep_{33}^2 \end{bmatrix}\right\}\begin{bmatrix} U_2 \\ U_6 \\ U_5 \end{bmatrix}\begin{matrix} \to U_1^2 \\ \to U_2^2 \text{ (not on boundary)} \\ \to U_3^2 \end{matrix} \tag{1b}$$

Since global node #6 is not on the boundary, hence no endpoint *ep* term is associated with U_6.

For e = 3, with only its node #3 not attached to the boundary.

$$\begin{bmatrix} 0 \\ 0 \\ 0 \end{bmatrix}=\left\{\begin{bmatrix} A_{11}^3 & A_{12}^3 & A_{13}^3 \\ A_{21}^3 & A_{22}^3 & A_{23}^3 \\ A_{31}^3 & A_{32}^3 & A_{33}^3 \end{bmatrix}+\begin{bmatrix} ep_{11}^3 & ep_{12}^3 & ep_{13}^3 \\ ep_{21}^3 & ep_{22}^3 & ep_{23}^3 \\ 0 & 0 & 0 \end{bmatrix}\right\}\begin{bmatrix} U_2 \\ U_3 \\ U_7 \end{bmatrix}\begin{matrix} \to U_1^3 \text{ (on boundary)} \\ \to U_2^3 \text{ (on boundary)} \\ \to U_3^3 \text{ (not on boundary)} \end{matrix} \tag{1c}$$

Since global node #7 is not on the boundary, hence no endpoint *ep* term is associated with U_7, so on and so forth. It can be easily observed that global nodes #6, 7, 10, and 11 will all eventually have no endpoint *ep* term associated with them.

In these latter three equations (1a) to (1c) above, for any particular row equation, say the j^{th} row for the e^{th} element [e^{th} equation, either (1a), (1b) or (1c)], it pertains to the testing (weighting) function $W(x,y) \overset{Galerkin}{=} N_j^e(x,y)$, and this $N_j^e(x,y)$ is exactly that in ep_{ij}^e of (2) above. However, only when this j^{th} node of this e^{th} element is on the boundary does this ep_{ij}^e of (2) come into play, i.e. non-zero, because it is the boundary term. But when this j^{th} node of this e^{th} element is not on the boundary, then ep_{ij}^e vanishes and does not come into play.

Therefore, of all the elemental matrix equations, only those row equations in the same row as U_6, U_7, U_{10}, and U_{11} remain unchanged, i.e. no ep_{ij}^e required to be added to them, while the rest: $\left[A_{ij}^e \quad A_{i,j+1}^e \quad A_{i,j+2}^e \right] \left[U_p \right]$, being a certain row equation in any one of the elemental matrix equations, in which p is neither 6, 7, 10, nor 11, must be changed to $\left[A_{ij}^e + ep_{ij}^e \quad A_{i,j+1}^e + ep_{i,j+1}^e \quad A_{i,j+2}^e + ep_{i,j+2}^e \right] \left[U_p \right]$.

Now, it is recalled that U_1, U_2, U_3, U_4, U_5, U_8, U_9, U_{12}, U_{13}, U_{14}, U_{15}, and U_{16} (all global boundary node values) vanish. Thus, for TM^z modes, the matrix equation on Pg 137 of the class slides is modified to

$$\begin{bmatrix} \begin{pmatrix} A_{22}^2 + A_{33}^4 + A_{22}^7 \\ + A_{11}^9 + A_{11}^{10} \end{pmatrix} & A_{32}^4 + A_{12}^9 & A_{23}^7 + A_{13}^{10} & A_{13}^9 + A_{12}^{10} \\ A_{23}^4 + A_{21}^9 & \begin{pmatrix} A_{33}^3 + A_{22}^4 + A_{33}^6 \\ + A_{22}^9 + A_{11}^{11} \end{pmatrix} & 0 & A_{23}^9 + A_{13}^{11} \\ A_{32}^7 + A_{31}^{10} & 0 & \begin{pmatrix} A_{33}^7 + A_{22}^8 + A_{33}^{10} \\ + A_{22}^{13} + A_{11}^{15} + A_{11}^{16} \end{pmatrix} & A_{32}^{10} + A_{12}^{15} \\ A_{31}^9 + A_{21}^{10} & A_{32}^9 + A_{31}^{11} & A_{23}^{10} + A_{21}^{15} & \begin{pmatrix} A_{33}^9 + A_{22}^{10} + A_{33}^{11} \\ + A_{33}^{12} + A_{22}^{15} + A_{11}^{17} \end{pmatrix} \end{bmatrix} \begin{bmatrix} U_6 \\ U_7 \\ U_{10} \\ U_{11} \end{bmatrix} = \begin{bmatrix} 0 \\ 0 \\ 0 \\ 0 \end{bmatrix} \qquad (3)$$

which can then be solved for U_6, U_7, U_{10}, and U_{11}, with the rest of the other 'U's already known to be zeros.

II. The Project

Consider a rectangular waveguide with cross sectional dimensions a x b, being the size along x and y respectively. The well-known cutoff wavenumber $k_{c,mn}$ of a particular $(m, n)^{th}$ mode is stated as

$$k_{c,mn} = \sqrt{\left(\frac{m\pi}{a}\right)^2 + \left(\frac{n\pi}{b}\right)^2}, \tag{4}$$

and the corresponding cutoff frequency is

$$f_{c,mn} = \frac{k_{c,mn}}{2\pi\sqrt{\mu\varepsilon}} \tag{5}$$

where m and n are integer modal indices, defining the number of half-cycle field variations along x and y respectively, and μ and ε are the permeability and permittivity of the medium filling the waveguide homogeneously.

You are provided with a MATLAB code that solves the eigenvalue problem of the rectangular waveguide whose cross section is meshed up into triangular facets as shown in Fig. 1 below. The associated node location and element connectivities are given in Tables I and II.

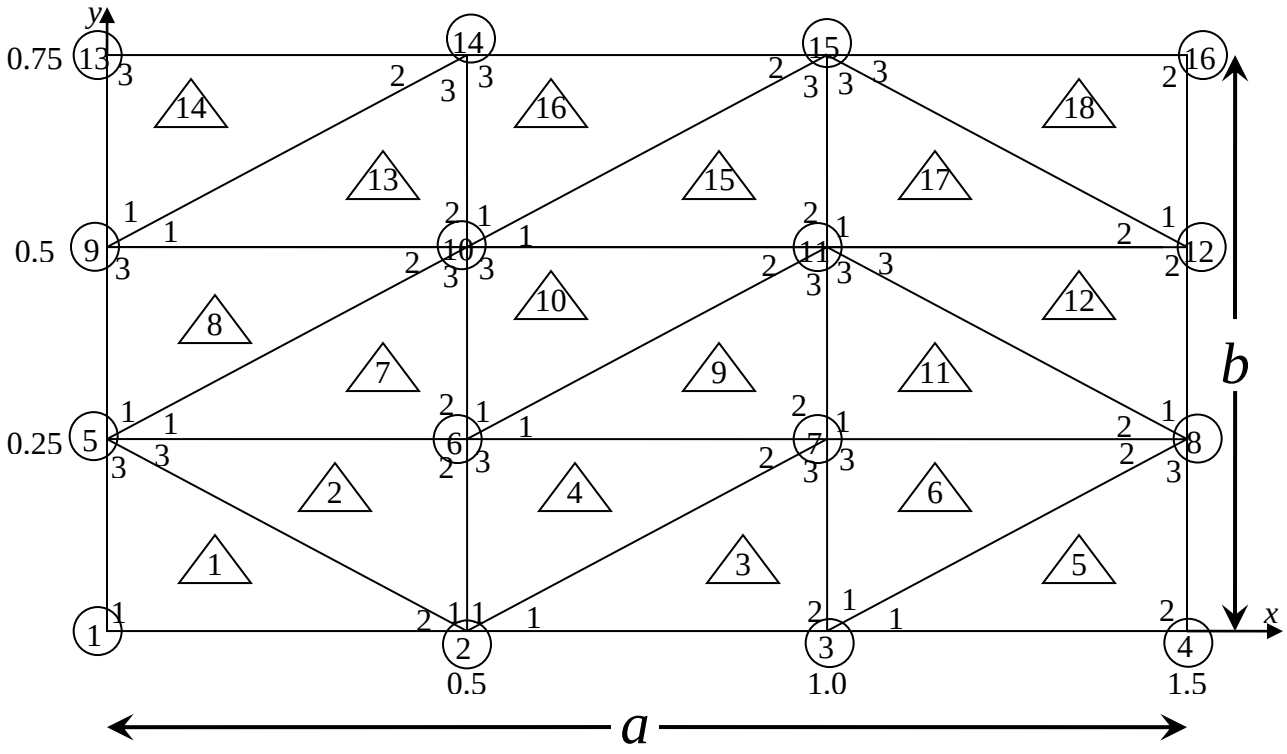

Fig. 1: Cross section of a rectangular waveguide meshed up into triangular facets

Table I: Triangle connectivity table

Element number e	Local node arrays		
	$n(1,e)$	$n(2,e)$	$n(3,e)$
1	1	2	5
2	2	6	5
3	2	3	7
4	2	7	6
5	3	4	8
6	3	8	7
7	5	6	10
8	5	10	9
9	6	7	11
10	6	11	10
11	7	8	11
12	8	12	11
13	9	10	14
14	9	14	13
15	10	11	15
16	10	15	14
17	11	12	15
18	12	16	15

Table II: Node location table

Global Node Number	x	y
1	0	0
2	0.5	0
3	1	0
4	1.5	0
5	0	0.25
6	0.5	0.25
7	1	0.25
8	1.5	0.25
9	0	0.5
10	0.5	0.5
11	1	0.5
12	1.5	0.5
13	0	0.75
14	0.5	0.75
15	1	0.75
16	1.5	0.75

Run the code and observe the graphs of the computed cutoff wavenumbers and cutoff frequencies over various modes as compared with the theoretical values. As will be seen, the agreement is fairly good for the first few dominant modes, but gets unacceptably poor for higher order ones. The reason for this is that an inadequate number of nodal points are considered in this code, being just 18. (Note that the dimensions a and b in the code may be arbitrarily set.)

Task 1: Rectangular Waveguide of Denser Mesh

Modify the given MATLAB code to treat a much higher density of mesh – in the order of at least 300 elements. You should construct the mesh on your own, for which the fashion of the arbitrary triangulation is up to you to define. Plot the corresponding graph of computed cutoff wavenumbers for various modes and demonstrate that with your finer meshing, the agreement of the computed cutoff wavenumbers and cutoff frequencies with theory is significantly improved. The waveguide dimensions a and b are up to you to set. In your report, in addition to the modified code and numerical results, the drawing of the new densely-meshed rectangle should be included, as well as the corresponding two tables of Tables I and II – the connectivity and node location tables.

Task 2: Extension to Ridge Waveguides

A ridge waveguide has a cross section designed to allow a single mode of propagation over larger bandwidths than a rectangular waveguide. A typical cross section of a ridge waveguide is shown in Fig. 2, whose outer dimensions a and b are as indicated, and the arbitrary factor $\kappa > 1$ defines the width of the center 'bridge' portion connecting the two side 'arms'.

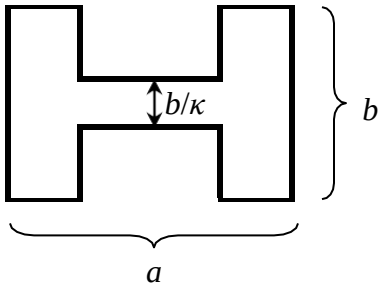

Fig. 2: Cross section of a ridge waveguide

Repeating the same as for the rectangular waveguide, write a modified code to treat the ridge waveguide with outer dimensions a and b being the same as those of the rectangular waveguide which you have chosen earlier, and having a bridge width defined by, say $\kappa = 3$. As before, ensure to use an adequate mesh density, at least around 300 elements in order to obtain reasonably accurate results. Likewise, include the mesh diagram of the ridge waveguide and the associated two tables in your report for this task.

Task 3: Compare Cutoff Frequencies

Compute the ratio f_{c1}/f_{c2} between the two lowest cutoff frequencies of the two lowest-order modes for both the rectangular waveguide and the ridge waveguide which you have investigated. Is the bandwidth larger for the ridge waveguide?

Your Report

Hand in your report before 2021/06/13.